Table 2 A_Y and ϕ follower loop parameters

Symbol	Final system	Flight system
$K_{\dot{\phi}c}$	0.5	0.7
K_{mY}	1.2	1.67
K_ϕ	0.8	0.77
G_ϕ	1	1
K_{AYA}	0.004 rad/fps^2	0.0038
G_{AYA}	$5s/(1+5s)$	$5s/(1+5s)$
K_{AY}	0.07 rad/fp^2	0.04
G_{AY}	1	1
K_P	0.2	0.17
G_P	1	1
$G_{ST\delta A}$	$(1+s/250)/(1+s/62.5)$	$(1+s/300)/(1+s/30)$
$G_{ST\delta R}$	$(1+s/400)/(1+s/250)$	$(1+s/300)/(1+s/125)$
K_R	1	0.8
G_R	$2s/(1+2s)$	$2s/(1+2s)$

V. Summary

The NF106B-VST modification and flight program provided an excellent opportunity to demonstrate the success of a comprehensive approach to design of a high performance flight control system. By using a planned iterative procedure it was possible to apply several complementary analytical techniques effectively, and to factor updated information into the problem readily. Emphasis was placed on developing a complete yet workable mathematical model including high frequency dynamics where data were available. This proved valuable in diagnosing and solving problems which arose during simulation and testing phases of the program. Pilot opinions and recorded flight test data indicated that the system resulting from the effort described in this paper performs very well.

References

[1] Wong, B., Burke, H., Hutton, M., and Farris, R., "NF106B-VST Model Follower and Structural Protection System Design," ER 14278, Feb. 1967, Martin Marietta Corp., Baltimore, Md.

[2] Teper, G. L. and Jex, H. R., "Feasibility of Using F-106B Aircraft for a Variable Stability Trainer," STI 136-1, March 1965, Systems Technology Inc., Hawthorne, Calif.

JUNE 1971 J. AIRCRAFT VOL. 8, NO. 6

Hover and Forward Speed Aerodynamics of Several Tracked Air-Cushion Vehicle Models

HENRY W. WOOLARD,* KWAN L. SO,* AND RICHARD J. SERGEANT†
TRW Systems Group, Redondo Beach, Calif.

Hover and moving-ground-plane wind-tunnel tests were performed on three elongated Tracked Air-Cushion Vehicle (TACV) models and one circular air-cushion model in a joint TRW-NASA Langley test program. Selected results are presented for all the models tested in hover and for one of the elongated models tested at forward speed. Separate force and moment measurements on the body and cushions were taken. The air-cushion lifting performance in hover was found to be influenced by cushion length-to-width ratio, cushion-jet Reynolds number, and body-shell proximity. At a fixed cushion height and constant air-flow rate, cushion lift generally increased with forward speed to a peak value and then decreased. This characteristic diminished with increasing cushion height. For the elongated model at forward speed, the body forces, and moments generally were greater than those of the cushion except for the lift and pitching moment.

Nomenclature

A_c = air-cushion base area
C_L = body lift coefficient, $L_b/q_\infty S_m$
C_m = body pitching-moment coefficient, $m_b/q_\infty S_m l_b$
C_p = pressure coefficient, $(p-p_\infty)/q_\infty$
d_m = diameter of a circle having an area equal to the body maximum cross-sectional area
h = air-cushion edge height
h^* = height parameter, $h/t(1+\sin\gamma)$ or $1/t^*$
H = total pressure (absolute)
$\bar{k}_B'$ = belt forward-speed parameter, $q_B/(\bar{p}_c-p_\infty)_o'$
$\bar{k}_F, \bar{k}_F'$ = air-cushion forward-speed parameter, $q_\infty/(\bar{p}_c-p_\infty)_o, \bar{q}_\infty/(\bar{p}_c-p_\infty)_o'$
$\bar{K}_c'$ = air-cushion mean-pressure parameter, $(\bar{p}_c-p_\infty)_o'/(H_p-p_\infty)$
K_Q = normalized air-flow rate [see Eq. (1)]
l = length
l = rolling moment about the x axis; positive, using a left-hand rule
L = lift force (see text)
L_k = air-cushion lift due to body cavity pressure, $(\bar{p}_c-\bar{p}_k)A_c$
L_M = lift measured by strain-gauge balance
$(L_c)_0$ = cushion lift in hovering state
m = pitching moment about an axis parallel to the y axis; positive, using a right-hand rule (see Fig. 1 for moment centers)
n = yawing moment about an axis parallel to the z axis; positive, using a left-hand rule (see Fig. 1 for moment centers)
p = static pressure (absolute)
$(\bar{p}_c-p_\infty)$ = air-cushion mean gauge pressure

Presented as Paper 69-750 at the CASI/AIAA Subsonic Aero- and Hydro-Dynamics Meeting, Ottawa, Canada, July 2–3, 1969; submitted July 11, 1969; revision received February 25, 1970. This work was supported by the Office of High Speed Ground Transportation, U.S. Department of Transportation, under Contract C-353-66(NEG). The technical contributions of K. J. Grunwald, D. Hammond, and R. E. Kuhn, participants for NASA, are gratefully acknowledged.

* Member of Technical Staff, Aerothermodynamics Department, Aerosciences Laboratory. Members AIAA.

† Member of Technical Staff, Aerothermodynamics Department, Aerosciences Laboratory.

$(\bar{p}_c - p_\infty)'$ = air-cushion mean gauge pressure uncorrected for jet-thrust lift‡ $(L_M - L_k)/A_c$
q = dynamic pressure or equivalent, $\rho U^2/2$
Q = cushion volumetric flow rate (ft³/sec)
S_m = body maximum cross-sectional area
t = jet-nozzle exit thickness
t^* = nondimensional nozzle thickness $(t/h)(1 + \sin\gamma)$ or $1/h^*$
$\bar{u}_j$ = mean velocity at nozzle exit
U = velocity
w = width
$\dot{w}$ = weight flow rate (lb/sec)
x,y,z = rectangular coordinates
Y,Y = force components parallel, respectively, to the x and y axes
β = angle of yaw
γ = inclination of jet-nozzle axis
ν = kinematic viscosity (ft²/sec)
ξ = periphery of air-cushion jet nozzle
π_{BA} = basic cushion power, $Q(H_p - p_\infty)$
π_{RC} = ideal ram-recovery power, $q_\infty Q$
π_{RD} = ram-drag power, $2q_\infty Q$
π_{TOT} = ideal total power, $\pi_{BA} + \pi_{RD} - \pi_{RC}$
ρ = air density (slugs/ft³)
$(\ )_b$ = denotes body
$(\ )_B$ = denotes ground-plane belt
$(\ )_c$ = denotes air cushion
$(\ )_k$ = denotes cavity region
$(\ )_o$ = denotes hover condition $(U_\infty = U_B = 0)$
$(\ )_p$ = denotes cushion plenum (except for C_p)
$(\ )_\infty$ = denotes free stream or ambient conditions
$(\bar{\ })$ = denotes a mean value
$(\ )'$ = denotes a quantity based on $(\bar{p}_c - p_\infty)_o'$

Introduction

PREVIOUS investigations dealing with the aerodynamics of air-cushion vehicles generally have been oriented toward low-speed untracked air-cushion vehicle configurations, and studies of the effects of relative motion of ground plane and vehicle are rather meager.[1] The present tests were taken to provide aerodynamic information for configurations more nearly representative of those anticipated for Tracked-Air Cushion Vehicles, and to determine the importance of ground-plane motion in the interpretation of wind-tunnel test results on these vehicles.

The test program was a cooperative effort of the TRW Systems Group and the NASA Langley Research Center for the Office of High Speed Ground Transportation. Wind-tunnel tests were performed over the moving-ground plane in the 17-ft test section of the 7- × 10-ft wind tunnel at the NASA Langley Research Center.

Illustrations of the air-cushion planforms and body air-cushion combinations tested are summarized in Fig. 1.§ The circular model shown is not intended to be representative of a Tracked Air-Cushion Vehicle, but is included as a basic shape for reference. A more detailed illustration of the VS6-CS3 model appears in Fig. 2. The CS1 and CS3 cushions each were tested in a peripheral-jet and a hybrid-plenum mode. These modes are associated with the position of the air-cushion base as shown in Fig. 3. The base in the hybrid-plenum mode is elevated $\frac{1}{2}$ in. above that for the peripheral-jet configuration.

Relative to a hypothetical full-scale vehicle, the elongated models of Fig. 1 are approximately $\frac{1}{15}$ full scale.

‡ The lift due to jet-thrust reaction has been shown[1] to be of the order of 2% or less of the total lift for the present tests.

§ The initials VS and CS denote a body and air-cushion configuration respectively in the alpha numeric designations appearing in Fig. 1. The numeric term denotes the specific model identified in the figure. A number in parentheses following a cushion designation indicates the number of cushions. A complete vehicle (body plus cushion) is denoted by VS6-CS3, for example, whereas a cushion alone is denoted by CS3.

Selected results only are presented. Some hover test data are given for each of the air cushions shown in Fig. 1. Forward-speed results are presented only for the VS6-CS3 model. More detailed information may be found in Ref. 1.

Test Facility

The forward-speed tests were conducted over the moving-belt ground plane in the 17-ft test section of the tandem-test-section 7-× 10-ft wind tunnel at the NASA Langley Research Center. The maximum usable moving ground speed is approximately 100 ft/sec. The facility is described in some detail by Turner.[2]

The NASA facility was designed for V/STOL testing and therefore did not provide the precise control and monitoring of the ground surface conditions required for TACV testing. The design height for peripheral-jet models tested was of the order of 0.10 in. The root-mean-square ground-plane surface variations therefore should be small compared to this dimension. The maximum variations in the moving belt thickness and the backing plate flatness were ±0.007 and ±0.010 in., respectively. The root-mean-square variations, which are smaller, are not available. During tests with the ground moving, additional variations in contour were introduced by a slight lifting of the ground-plane belt. The lifting displacement of the belt is not known exactly since an attempt to measure it was unsuccessful. It is estimated, however, that it was of the order of 0.02 in.

Models and Instrumentation

An illustration of the principal model installation features for the VS6-CS3 model appears in Fig. 2. The CS3 air-cushion configurational details are generally typical of the other elongated air cushions. The model body shells were of a molded fiber-glass construction and the air-cushion assemblies of an aluminum alloy construction.

The air-cushion nozzle geometry is illustrated to scale in Fig. 3. Specific geometric details are given in Ref. 1. Conversion from one cushion mode to the other was accomplished by means of appropriately dimensioned spacers (see Sec. A-A of Fig. 2) in the plenum chamber. The peripheral-jet nozzle inclination was 30° from the vertical with a 10°-in. cluded angle of convergence.

The nozzle-exit thickness t should be sized from scaling considerations and consideration of the optimum thickness for minimum cushion-related power in the forward-speed condition. For a loss-free cushion air-supply system and a forward-speed parameter k_F of unity, it is shown in Ref. 1 that the value for t^* for minimum power in the forward-speed condition is $t^* = 0.312$. For $\gamma = 30°$, this yields a value of $t/h = 0.208$. Scaling considerations should then determine the thickness t. The models in these tests are approximately $\frac{1}{15}$ full scale. If it is assumed that the operating height for the full-scale vehicle is 1 in. (lower heights are under consideration), the design operating height for the model would be 0.067 in. This was considered to be too low in view of the previously mentioned variations in the ground surface conditions. A compromise design height of 0.100 in. was therefore selected. This yields a nozzle design thickness of 0.021 in. for the peripheral-jet cushion mode. A value of 0.30 in. was utilized for the hybrid-plenum mode. Measured mean nozzle thicknesses on the finished models are noted on Fig. 1 for both cushion modes.

Provision was made for separate measurement of the body air-cushion forces and moments. The strain-gauge balances for these purposes are identified in Fig. 2.

All the air-cushion models were provided with pressure taps on the cushion base and at selected points in the plenum chamber and nozzle passage. The VS6 body shell was provided with exterior surface pressure taps.

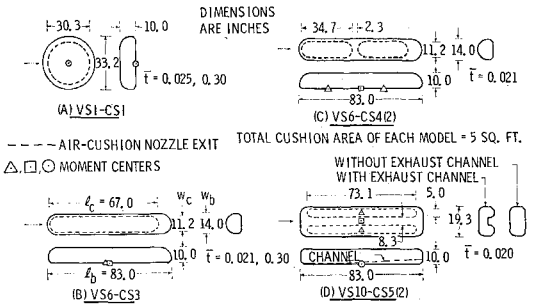

Fig. 1 Model configurations tested.

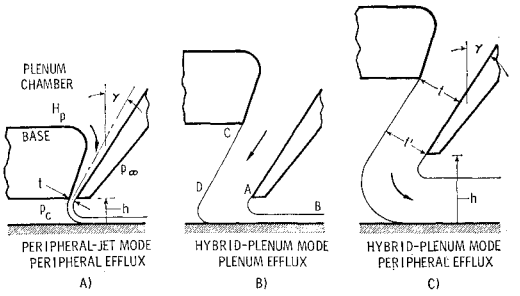

Fig. 3 Cushion modes and efflux regimes.

Discussion of Test Results

Hover Tests

For the hover state, the models were tested both in the wind tunnel and over an exceptionally smooth and flat surface in a "static room" test area outside the wind tunnel. The static-room tests, which were more comprehensive, will be presented here. These tests were performed on the air cushions both with and without the body shell present. It was found[1] that the air-cushion mean-pressure parameter $\bar{K}_c'$ was reduced by the presence of the body shell. In general, the reduction was of the order of 10% at a cushion height of 0.10 in. and decreased to zero as the height increased to 0.40 in. For the sake of clarity, only those results for the air cushions without a body shell will be presented.

The tests of Ref. 1 also revealed a jet Reynolds number influence on the air-cushion pressure parameter. An illustration of this influence for constant cushion heights and constant cushion lift values is shown in Fig. 4 for the peripheral-jet CS3 cushion. Note the difference in the variation of the cushion-pressure parameter with height at a constant lift and at constant half-jet Reynolds number. This characteristic should be borne in mind when comparing test data.

A theoretical analysis of the effect of convergent-nozzle viscous losses on peripheral-jet performance was developed by the present authors in Ref. 1. As will be seen later, the degree to which this analysis agrees with experiment depends upon the cushion length-to-width ratio. However, in all cases, the theoretical curves of pressure parameter as a function of Reynolds number for a constant cushion height are almost identical in shape to the experimental curves (e.g., Fig. 4), but are displaced from them by a constant amount. The displacement constant is a function of height and cushion shape.

The paired-cushion data were used in some cases to estimate the length-to-width ratio effect for single cushions. For the parallel cushions, CS5(2), it was found that there was no interference between cushions. The foregoing procedure was therefore acceptable, and an average value for the two cushions was used. The interference between cushions for the tandem cushion model CS4(2) was not determined. Nevertheless, the individual cushion-pressure parameters (with both cushions operating) were averaged and taken to be representative of the isolated single-cushion performance. Considering the flow scale for the tandem model (the jet thickness was 0.021 in. with a minimum distance of 2.3 in. between jets), it is believed that the interference between cushions was probably small.

Before presenting the hover test data, a comment regarding the behavior of the hybrid-plenum air cushion is perhaps worthwhile. The hybrid-plenum cushion was so named because it was hypothesized that at very low heights ($h \ll t$) the efflux (see Fig. 3b) from the edge of the cushion would be similar to that from a plenum air cushion, whereas, at heights of the order of, or greater than, the nozzle thickness, the efflux would be similar to that from a peripheral jet with a rigid outer skirt (Fig. 3c). It was found in Ref. 1, however, that at low heights the use of a pseudo peripheral-jet theory for the hybrid-plenum cushion yielded better agreement with experiment than did plenum theory. The pseudo theory was based on the assumption that the emergent stream from the nozzle in Fig. 3c flows along the skirt atcons tant thickness so that $t = t'$. In subsequent comparisons, the hybrid-plenum cushion-height parameter is determined on this basis.

A comparative plot of the cushion-pressure parameter as a function of the height parameter h^* for the various cushions at a constant cushion lift of approximately 20 lb, is presented in Fig. 5. Also shown in this figure are the exponential-theory[1] curve, and the viscous theory[1] curve for a 0.021-in. thick nozzle. It is seen in the figure that the pseudo peripheral-jet concept appears to correlate the hybrid-plenum performance with the peripheral-jet performance. Correlation cannot be claimed with certainty since test points for overlapping values of the height parameter for the two cushion modes are not available.

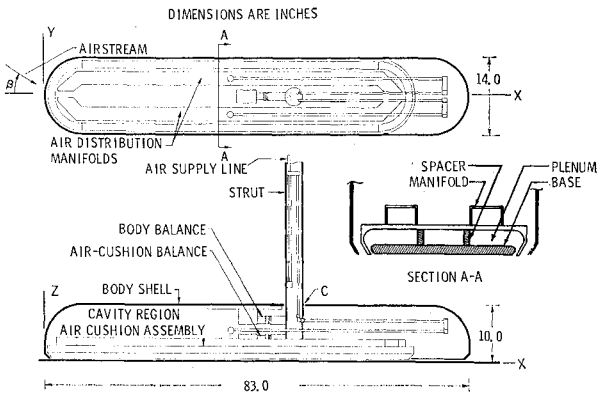

Fig. 2 The VS6-CS3 model and coordinate system.

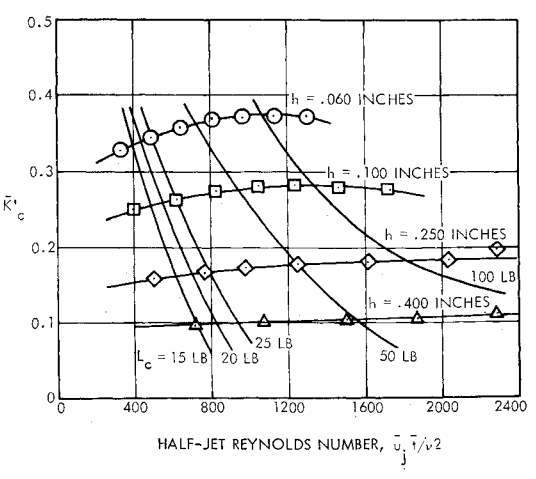

Fig. 4 Cushion-pressure parameter as a function of half-jet Reynolds number for the peripheral-jet CS3 cushion in hover.

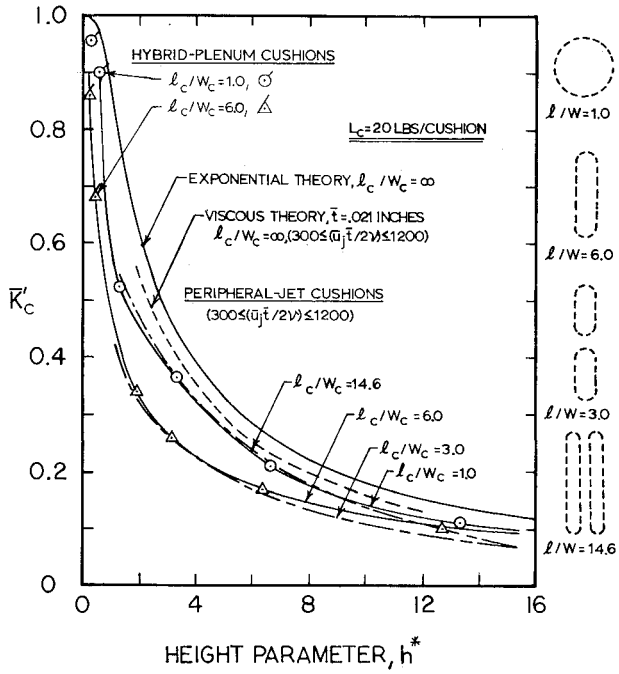

Fig. 5 Cushion-pressure parameter as a function of the height parameter at constant lift for the CS1, CS3, CS4(2), and CS5(2) cushions in the hover state.

Cross-plots of the curves of Fig. 5 using the cushion length-to-width ratio as the independent variable are shown in Fig. 6. The systematic influence of cushion height and length-to-width ratio is apparent in the latter figure. It is seen that the experimental cushion pressure parameter for circular and very high length-to-width ratio cushions tends toward the inviscid theoretical values. It is observed in Fig. 5 that the difference between theory and experiment for these planforms is even smaller when nozzle viscous-flow losses are taken into account. That is, nozzle viscous-flow losses account for a substantial portion of the difference between inviscid theory and experiment for those cushions for which the length-to-width ratio effects are small.

The normalized air flow rate K_Q is defined as

$$K_Q \equiv Q(h\xi/1+\sin\gamma)^{-1}(H_p-p_\infty/\rho/2)^{-1/2} \qquad (1)$$

This parameter, as a function of the height parameter for the various cushions, is presented in Fig. 7. The experimental air-flow rate test points correlate well among themselves and fairly well with the Barratt theory, except near $h^* = 0.50$. Exponential and Barratt theories[1] yield essentially identical values of K_Q for h^* greater than 0.6. However, for $h^* =$ 0, K_Q is unity and infinity, respectively, for the exponential and Barratt theories.

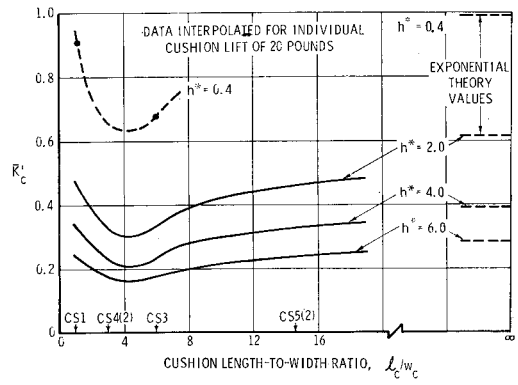

Fig. 6 Effect of cushion length-to-width ratio on the air-cushion mean-pressure parameter at constant lift in the hover state.

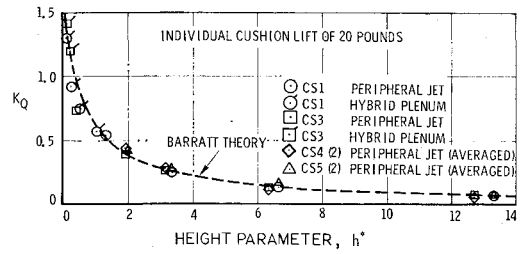

Fig. 7 Normalized air-flow rate as a function of the height parameter at constant lift for the CS1, CS3, CS4(2), and CS5(2) cushions in the hover state.

Forward-Speed Tests

As mentioned previously, selected results are presented only for the VS6-CS3 model. More detailed information on the VS6-CS3 tests and the results for the other models may be found in Ref. 1.

An objective of the forward-speed tests was the determination of whether a moving-ground plane is necessary for valid TACV wind-tunnel test results. For this objective, a number of identical runs were made for the ground plane both moving and stopped. For those runs made with the airstream on and the ground plane moving, the ground-plane speed always matched the airstream velocity.

Yaw tests were run in an attempt to simulate a side wind. Tests were conducted for the ground plane both moving and stopped. Neither case is a true simulation, since in the real situation the relative ground motion is parallel to the vehicle's longitudinal axis. However, the results are believed to be useful in establishing the general order of the side-wind effects, particularly for the vehicle body.

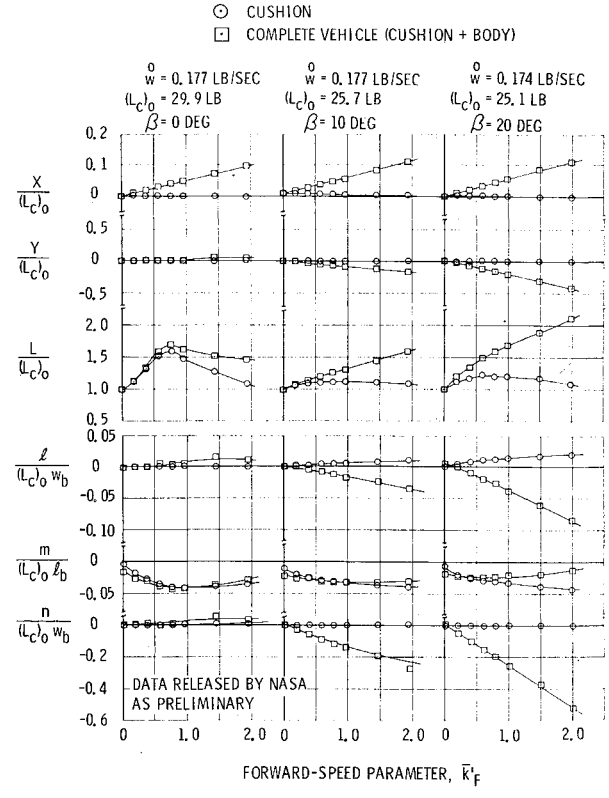

Fig. 8 Vehicle (cushion plus body) and cushion-aerodynamic characteristics at forward speed (ground plane moving) for the peripheral-jet VS6-CS3 model at h = 0.100 in.

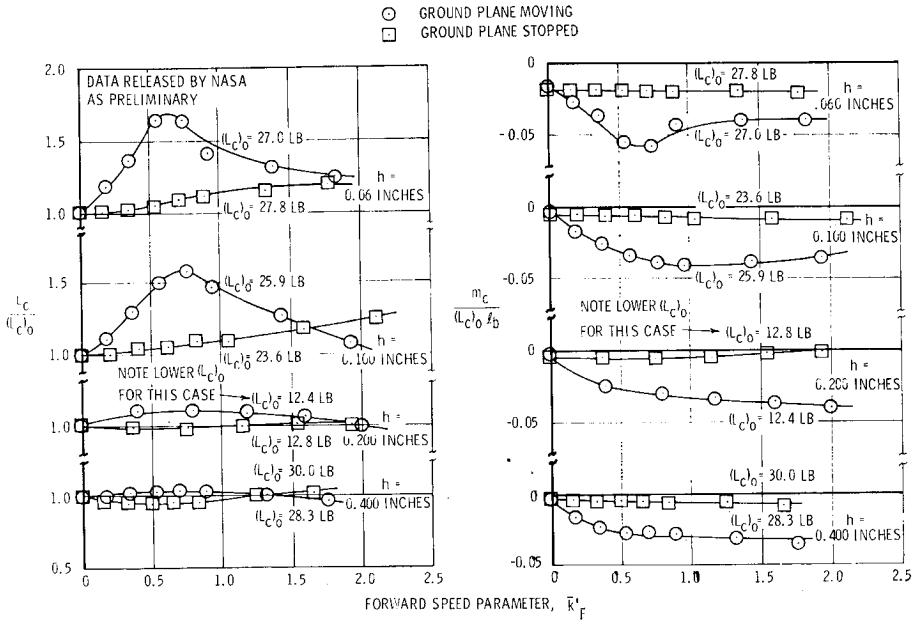

Fig. 9 Effect of ground motion on cushion lift and pitching moment at forward speed for the peripheral-jet VS6-CS3 model at constant-cushion air flow and zero yaw.

For an actual vehicle, the condition of restraint for a trip between two terminals is a constant lift, assuming no change in vehicle weight due to fuel consumption. It is therefore desirable to conduct wind-tunnel tests at this condition, or, alternatively, to obtain enough test points to cross-plot the data to a constant lift condition. Practical considerations prohibited application of either approach. The procedure followed was to maintain, as the airstream velocity varied, a constant cushion air-weight flow rate corresponding to a specified cushion hover lift $(L_c)_o$. Most of the data were taken at a nominal cushion hover lift of 25 lb.

The exact cushion heights during a run with the ground plane moving are not known, since the instrumentation installed for this purpose failed to give reliable data. The cushion heights given in the data are for the hover state. Since there was a tendency for the belt to lift away from the backing plate, the actual heights were probably slightly smaller. Although the lifting displacement of the belt is not known exactly, it is believed to have been of the order of 0.02 in.

During the tests the static pressure in the body-shell cavity (see Fig. 2) was lower than ambient pressure. The body and cushion lift forces measured directly by the balances were therefore relative to this pressure. When individual body and cushion lift forces or coefficients are presented herein, however, they are adjusted to a standardized value based on the assumption that freestream static pressure exists in the body-cavity region.

The complete vehicle (cushion plus body) and air-cushion aerodynamic characteristics as functions of the forward-speed parameter for the peripheral-jet VS6-CS3 model at constant yaw angles, a hover lift of approximately 25 lb, a height of 0.100 in., and the ground plane moving, are given in Fig. 8. The same aerodynamic characteristics for both cushion modes, several heights, and ground plane moving and stopped are presented in Ref. 1.

It is apparent from the figure that the body forces and moments dominate for all characteristics but the lift and pitching moment. At zero yaw angle, the cushion lift and pitching moment definitely dominate. At a yaw angle of 20° and a forward-speed parameter greater than about 1.5, the cushion and body lift and pitching moment are of about the same order of magnitude.

The foregoing characteristic regarding the relative distribution of forces and moments between the body and cushion is typical for both cushion modes, and for both ground-plane conditions; the detailed behavior differs, however, for the different cases.

The development of body lift with forward speed, and body lift, side force, rolling moment, and yawing moment with yaw angle exhibited in Fig. 8 is significant to the stability and control characteristics of an actual vehicle. Aerodynamic characteristics for other body shapes without air cushions are given by Grunwald.[3] Woolard[4] has theoretically calculated side-wind effects for ground vehicle bodies of semielliptic cross section.

Another noteworthy characteristic exhibited in Fig. 8 is the air-cushion lift behavior at zero yaw angle for the ground plane moving. With increasing forward speed, the cushion lift rises rapidly to a peak value and then decreases to a value near the hovering lift.

The foregoing characteristic is displayed more graphically in Fig. 9 which shows the effect of ground-plane motion on the air-cushion normalized lift¶ and pitching moment as functions of the forward-speed parameter at zero yaw angle and several heights. The corresponding curves for the hybrid-plenum cushion mode are given in Ref. 1.

The fact that ground-plane motion is responsible for the lift peak is clear in this figure.

It is seen in the figure that the lift peak disappears at the higher heights. It is also seen that the lift rise is accompanied by an increasingly negative pitching moment.

For the hybrid-plenum mode, the variation of the lift peak with height differs from the peripheral-jet case, in that a height for a minimum peak appears to exist. A direct comparison of the two-cushion modes appears in Fig. 10 for the ground plane moving. It is seen that the hybrid-plenum cushion achieves a higher-lift peak $[L_c/(L_c)_o = 1.9]$ than does the peripheral-jet cushion.

The magnitude and extent of the foregoing lift-peaking characteristic varies with the hover lift magnitude. Curves showing this effect are presented in Ref. 1. In general, as the hover lift increases, the peak decreases in magnitude and occurs at a lower value of the forward-speed parameter.

Additional visibility on the source of the lift peak due to forward speed is provided in Fig. 11. Figure 11 shows the effect of ground-plane motion on the air-cushion normalized lift and pitching moment with the airstream on and off for the peripheral-jet and hybrid-plenum modes for a height of 0.100 in. The outstanding characteristic displayed in this figure is the behavior for the ground plane moving and the airstream off. Although the detailed behavior is somewhat different

¶ The hover lift $(L_c)_o$ was inadvertently set at approximately 12 lb for $h = 0.200$ in.

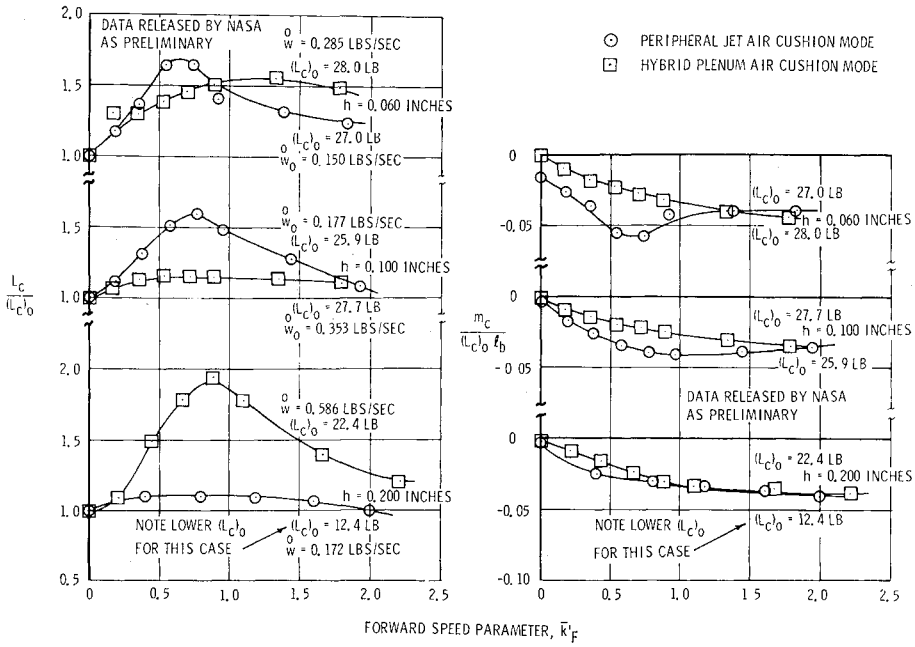

Fig. 10 Comparison of peripheral-jet and hybrid-plenum cushion lift and pitching moment at forward speed (ground plane moving) for the VS6-CS3 model at constant-cushion air flow and zero yaw.

for the two-cushion modes, both modes achieve high-lift values due to ground-plane motion alone. The negative pitching moment for both cases also is due almost entirely to ground-plane motion alone. These effects are believed to be a consequence of the cushion-bottom flow. Ground plane belt lifting could be a contributing factor, but this is not a known certainty.

Woolard, So, and Sergeant[1] theoretically analyzed cushion-bottom flow with the airstream off for a two-dimensional model which neglected the flow details at the cushion ends and assumed that the Reynolds equation for lubrication theory was applicable (although the test Reynolds number slightly exceeded the required magnitude). The analysis, which is applicable only to the peripheral-jet cushion mode, is incapable of producing quantitative results, but it did agree qualitatively with airstream-off behavior of Fig. 11.

It is seen in Fig. 11 that the application of the airstream in the case of the peripheral-jet cushion provides an additional lift increment up to a forward-speed parameter of 0.75. For higher values, the lift decreases. A possible explanation for this behavior follows. At low values of the forward-speed parameter, there is little or no deterioration of the peripheral-jet performance in the vehicle nose region. The jet is therefore capable of sustaining across its boundaries a pressure differential approximately equal to that for the airstream off. However, since the local external nose pressures (near the stagnation point) are higher with the airstream on, the cushion-base nose pressures are also higher, thereby generally elevating the cushion-base pressure level and increasing the lift. At higher values of the forward-speed parameter, the freestream air penetrates the cushion base causing a deterioration of the flow that leads to a lift decrease.

As seen in Fig. 11, the hybrid-plenum cushion behaves differently; it immediately experiences a loss in lift on application of the airstream. An explanation for this behavior is not forthcoming at this time.

Normalized centerline cushion-base pressure distributions for the peripheral-jet VS6-CS3 model with cushion power on and off, ground plane moving and stopped, airstream on and off, are shown in Fig. 12 for a cushion height of 0.100 in. The corresponding curves for the hybrid-plenum cushion are available in Ref. 1. The freestream velocity of 58 fps

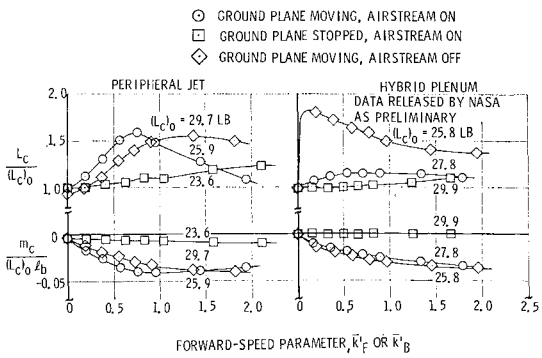

Fig. 11 Effect of ground-plane motion on cushion lift and pitching moment with airstream on and off at constant-cushion air flow for the VS6-CS3 model in both cushion modes at zero yaw and h = 0.100 in.

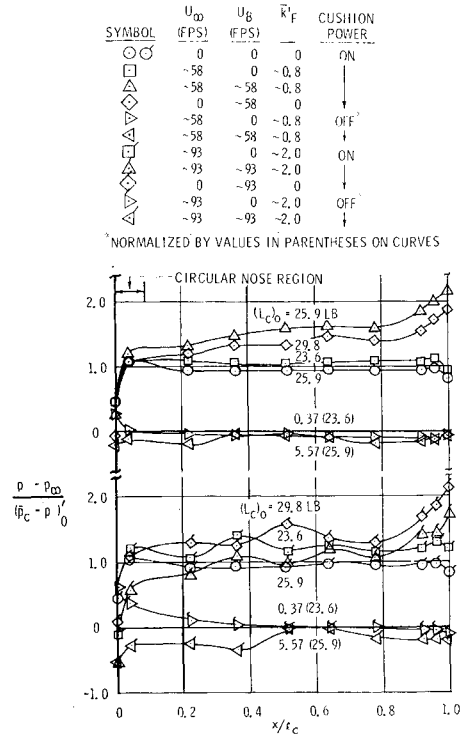

Fig. 12 Centerline cushion-base pressure distributions on the peripheral-jet VS6-CS3 model for cushion power on and off, ground plane moving and stopped, airstream on and off at zero yaw, and h = 0.100 in.

corresponds to the lift peak observed in the previous figures for $(L_c)_o = 25$ lb. The velocity of 93 fps is the maximum attainable in the tests.

The centerline longitudinal-pressure distribution for the peripheral-jet mode (Fig. 12) exhibits characteristics that might be expected on the basis of the previous lift and pitching-moment curves and the bottom-flow analysis of Woolard, So, and Sergeant.[1] The pressure distribution for the airstream-off condition with the belt moving at 58 fps, for example, exhibits the anticipated positive pressure gradient and the higher level indicative of the higher lift and increased negative pitching moment observed in Fig. 11. The lift change accompanying the application of the airstream is also evident in the pressure distribution.

The centerline cushion pressure distributions for the airstream-off condition with the belt moving at 93 fps exhibits a smaller positive pressure gradient than does the 58 fps case. This is believed to be due to the fact that the belt drags more air past the forward jet at the higher speed. The bottom-flow analysis of Woolard, So, and Sergeant[1] indicates that the larger the mass flow under the cushion, the smaller the pressure gradient becomes.

At zero yaw, the cushion-base lateral pressure distributions, which are not shown here but are available in Ref. 1, displayed a relatively flat characteristic aft of the circular nose region. In the nose region, they were parabolic in shape.

The effect of cushion type, ground-plane motion and cushion power on the body-aerodynamic characteristics as functions of the forward-speed parameter for the VS6-CS3 model are shown in Fig. 13. It is seen in the figure that the largest effect is on the lift coefficient as a consequence of ground-plane motion and the application of cushion power. Approximately the same phenomenon occurs for both the hybrid-plenum and peripheral-jet modes. The pitching moment is also affected.

It is observed that for the cushion power off, the body-lift coefficient is relatively independent of whether the ground plane is moving or stopped. However, with power on and the ground plane moving, a large loss in lift occurs at low values of the forward-speed parameter. Basically, the body-lift degradation occurs with the application of cushion power with the ground plane moving. It might be conjectured that the body-lift degradation at low forward speeds is caused by the cushion forward efflux dominating the oncoming free stream and thereby affecting the flow over the body; that is, the cushion is operating in the subcritical flow regime.[5] If this were the cause, however, a similar behavior (but of different magnitude because of the ground boundary layer

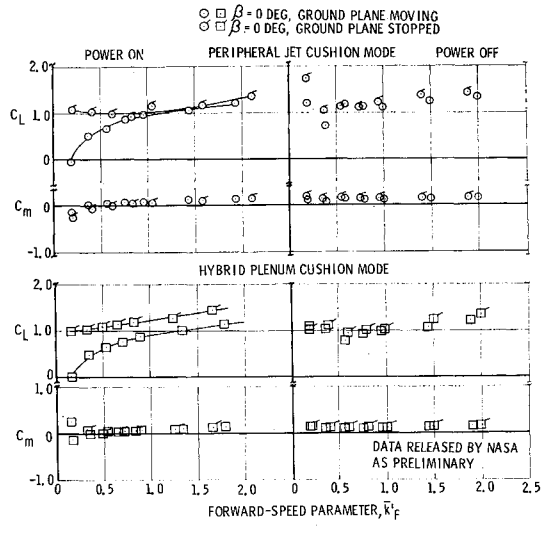

Fig. 13 Effect of cushion type, ground-plane motion, and cushion power on the body lift and pitching moment coefficients at forward speed, and constant-cushion air flow for the VS6-CS3 model at zero yaw, and $h = 0.100$ in.

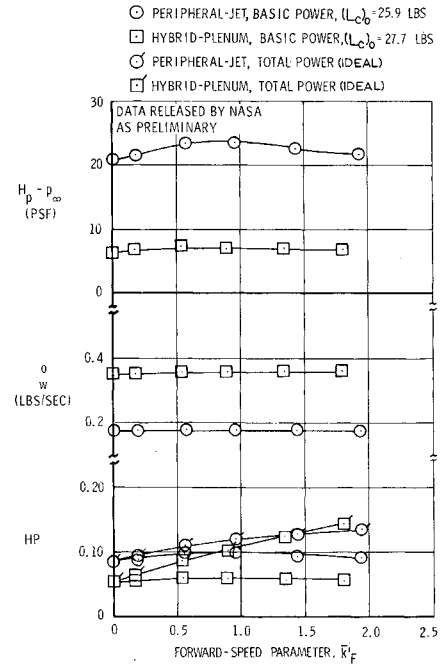

Fig. 14 Plenum total pressure, air-flow rate, and cushion horsepower at forward speed (ground plane moving) for the VS6-CS3 model at zero yaw and $h = 0.100$ in.

should be experienced for the ground-plane fixed condition. Since it is seen in Fig. 13 that this does not occur, the source of the loss in body lift remains to be determined.

The plenum-chamber total pressure, air-weight flow, cushion basic horsepower, and cushion ideal total horsepower (see nomenclature) as functions of the forward-speed parameter at zero yaw for the VS6-CS3 model in both cushion modes for the ground plane moving are shown in Fig. 14 for a height of 0.100 in. The basic power for the peripheral-jet mode is the larger at all speed parameter values shown. In the case of the total power, however, the peripheral-jet power is greater for speed parameter values below 1.4, whereas the hybrid-plenum power is greater for values above 1.4. The hybrid-plenum total power ultimately exceeds that of the peripheral-jet as the forward speed increases due to a greater rate of increase in ram-drag power; the rate is proportional to the air-weight flow, which is greater for the hybrid-plenum cushion.

Conclusions

The forward-speed test results presented were conducted at model heights considerably lower than those for which the NASA-Langley moving-belt facility was designed. Consequently, the ground-plane conditions were not as well controlled nor as well defined as might be desired. Possible implications of the foregoing limitations on the conclusions which follow should be borne in mind.

The test results indicate that the cushion-pressure parameter in the hover state for both peripheral-jet and hybrid-plenum cushions is influenced by cushion length-to-width ratio. At a constant lift, as the length-to-width ratio increases from unity, the pressure parameter at first decreases from a value near the theoretical to a minimum value and then increases asymptotically toward the inviscid theoretical two-dimensional value. The degree of influence of length-to-width ratio diminishes with increasing cushion height.

The hover tests demonstrated an influence of jet Reynolds number on the air-cushion pressure parameter. Deviations of the order of 10–15% in the pressure parameter are experienced for a half-jet Reynolds number variation from 500–1500. The pressure parameter increases with increasing Reynolds number.

An analysis for the effect of nozzle losses on the air-cushion pressure parameter accounted for a substantial portion of the difference between theory and experiment for those models for which the length-to-width ratio effects were small. The analysis also predicted a Reynolds number variation in agreement with experiment.

The hover tests indicated that the presence of an encapsulating shell about the air cushion generally deteriorated its performance at low cushion heights.

The forward-speed tests indicate that a moving-ground plane probably is needed for acceptable wind-tunnel results.

In general, the moving ground induced a positive longitudinal pressure gradient on the cushion base which contributed a negative pitching moment to the cushion. This characteristic was qualitatively verified by an approximate theoretical analysis of the effect of ground-plane motion on the cushion-bottom flow.

At forward speed, the moving ground was responsible for cushion lift increases in excess of the hover lift, the exact magnitude of the increase being dependent on cushion mode and the magnitude of the hover lift. In general, the cushion lift increased with forward speed until a peak value was reached.

For further increases in speed, the lift diminished with speed, but generally remained above the hover lift for most of these tests. This characteristic diminished with increasing height. For speeds below the peak lift, the moving ground was responsible for a major portion of the lift increase, although some contribution was obtained from the airstream. For speeds above the peak lift, the airstream was responsible for diminishing the lift.

For the single cushion elongated model utilizing both hybrid-plenum and peripheral-jet cushions, the hybrid-plenum cushion tended to perform like the peripheral one although there is not a well-defined pattern of behavior for the hybrid case. For speed parameter values below 1.4, the hybrid-plenum cushion required the lesser total power, whereas for speed-parameter values above 1.4, the reverse was true.

For the single cushion elongated model, with cushion power off, the body lift coefficient is relatively independent of whether the ground plane is moving or stopped. With cushion power on and the ground plane moving, however, a large loss in lift occurs at low values of the forward-speed parameter. It is hypothesized that the lift degradation is caused by the cushion forward efflux dominating the flow at the low forward speed. That is, the cushion is operating in what is commonly called the subcritical flow regime.

For elongated vehicles, the body forces and moments generally dominate over those of the cushion for all characteristics but the lift and pitching moment. Near zero yaw angle, for the ground plane moving, the cushion lift and pitching moment dominate, whereas at the higher yaw angles, the body lift dominates, and the cushion and body pitching moments are usually equally influential.

References

[1] Woolard, H. W., So, K. L., and Sergeant, R. J., "Moving Ground-Plane Wind-Tunnel Tests on Several Tracked Air Cushion Vehicle (TACV) Models," TRW Rept. 06818-6032-RO-00, March 1969, Redondo Beach, Calif. (PB 183857).

[2] Turner, T. R., "A Moving-Belt Ground Plane for Wind-Tunnel Ground Simulation and Results for the Two Jet-Flap Configurations," TN D-4228, Nov. 1967, NASA.

[3] Grunwald, K. J., "Aerodynamic Characteristics of High Fineness Ratio Vehicle Bodies at Cross-Wind Conditions in Ground Proximity," Working Paper 490, Oct. 10, 1967, NASA Langley.

[4] Woolard, H- W., "Slender-Body Aerodynamics for High-Speed Ground Vehicles," AIAA Paper 70-139, New York, 1970.

[5] Walker, N. K., "Some Notes on the Lift and Drag of Ground Effect Machines," *Proceedings of the National Meeting on Hydrofoils and Air Cushion Vehicles*, Institute of Aerospace Sciences, 1962.

JUNE 1971 J. AIRCRAFT VOL. 8, NO. 6

Graphite-Epoxy Wing for BQM-34E Supersonic Aerial Target

EDWARD J. MCQUILLEN* AND SHIH L. HUANG†
Naval Air Development Center, Warminster, Pa.

A graphite-epoxy composite wing has been analytically synthesized and designed. The objectives of this program were to exploit the improved properties of advanced fiber reinforced composites for primary structure of high-performance airborne vehicles, to extend structural mechanics technology to these nonisotropic, nonhomogeneous materials, and to gain service experience with no risk to human life. A computerized iterative design-analysis approach was used to minimize weight subject to both strength and flutter constraints. The wing is of sandwich construction with graphite-epoxy laminate skins bonded to aluminum honeycomb. The weight reduction was 50%.

Nomenclature

a_i = thermal expansion coefficient; $i = 1,2,6$
C_{ij} = stiffness matrix element; $i,j = 1,2 \ldots 6$
EI = bending rigidity
GJ = torsional rigidity
$h_L^{(k)}$ = distance from midplane to lower surface of kth ply
$h_u^{(k)}$ = distance from midplane to upper surface of kth ply
I = section mass moment of inertia
K_i = bending and torsional curvature of laminate; $i = 1,2,6$
M = mass
M_i = stress couple; $i = 1,2,6$
N_i = stress resultant; $i = 1,2,6$
n = total number of plies

Presented at the AIAA/ASME 11th Structures, Structural Dynamics, and Materials Conference, Denver, Colo., April 22–24, 1970; submitted May 21, 1970; revision received November 23, 1970. This paper represents results of in-house effort under Independent Research. Acknowledgment is made to the other members of the Applied Mechanics Research Group at the Naval Air Development Center who participated in this program. In particular A. Somoroff and T. Neu and H. Rubin made substantial contributions to the over-all effort.

* Head, Applied Mechanics Research Group, Aeromechanics Department. Member AIAA.
† Aerospace Engineer, Applied Mechanics Research Group, Aeromechanics Department.